Fabrication of ZnO Nanorods Structure for Drastically Enhancing Gas Sensing Response to NO₂ Gas

Nabeel Abood[1,2], Pradip Sable[1], Jamil Yassen[1] and Gopichand Dharne[1,*]

[1]Department of Physics, Dr Babasaheb Ambedkar Marathwada University, University Campus, Aurangabad Maharashtra 431004, India
[2]Faculty of Education Yefea, Aden University, Aden 6312, Yemen

(*Corresponding author's e-mail: drgmdharne@gmail.com)

Abstract

In this report, zinc oxide thin film was successfully deposited on a glass substrate by using a simple and low-cost technique i.e. modified Successive Ion Layer Adsorption and Reaction (SILAR). Prepared zinc oxide thin film was characterized for its physical and chemical properties by using XRD diffraction, Field Emission Scanning Electron Microscopy (FESEM), energy dispersive spectroscopy (EDS), UV-VIS spectroscopy, Raman spectroscopy and Fourier transform infrared spectroscopy (FTIR). The results of structural and morphological properties show that the prepared film has wurtzite hexagonal structure with nanorods-like morphology. Gas sensing characteristics revealed that the prepared film was sensitive to NO₂ gas. The response calculated at operating temperature 200 °C, was 1.37 when NO₂ concentration was 10 ppm, the response increased when the NO₂ concentration increased which reached to 2.16 when NO₂ concentration was 80 ppm with short response and recovery time.

Keywords: Thin film, ZnO, NO₂ gas, Nanorods, Gas sensing, Modified SILAR

Introduction

With the advancement of mankind in technology, the rapid industrial pollution resulting from the emission of toxic gases into the air such as carbon monoxide, carbon dioxide, methane and nitrogen oxide increases, so the need for air quality increases throughout the world. Among these gases, nitrogen dioxide is the most common, as it is produced by combustion in power plants, which leads to the formation of (ozone), which is a major component of smog and causes reduced lung capacity and a major cause of acid rain. NO_2 is a reddish-brown toxic gas with a pungent odor with a Threshold Value (TLV) of 3 ppm [1-3].

In order to detect such toxic gases, many researches have been conducted to obtain more sensitive sensors to detect gases that cause harm of the environment and humans. Among the different types of gas sensors, semiconductor metal oxide gas sensors are one of the most important sensors used to detect of toxic gases such as nitrogen dioxide gas (NO_2), which works on the principle of change of its electrical resistance upon contact of gas molecules with its surface [4]. Out of various semiconductor metal oxides used as sensing materials; ZnO nanostructure has been attracting more attention for using as sensing materials, due to its response to different gases and high stability [5,6].

Kaur *et al.* study the sensing properties of ZnO thin films prepared by Successive Ion Layer Adsorption and Reaction (SILAR). They found that the ZnO films exhibited highly sensitive, selective, low detection limit and short response/ recovery time (11/ 44 s) towards NO_2 gas for 20 ppm concentration [7]. Wang *et al.* prepared 3 different structures of ZnO (nanorods/flowers/spheres) by using the facile hydrothermal method, they found the ZnO nanospheres show the highest response to low concentration of NO_2 gas (5 ppm), while the ZnO nanorods exhibit the fastest response and recovery times (9 and 18 s to 5 ppm NO_2), respectively [8].

Various ZnO nanostructures and morphologies like nanorods, thin films, nanowires, nanoflowers, nanoplates, nanospheres, nanotubes, nanofibers, nanoneedles, nanobelts, quantum dots and nanoribbons [9-11], have been synthesized by applying different physical and chemical methods including chemical vapour deposition, (RF) sputtering, hydrothermal, Sol-gel methods [9], pulsed laser deposition [12], spray pyrolysis [13], electrochemical deposition [14], chemical bath deposition [15], and SILAR deposition [16]. Among of chemical methods, the SILAR has many advantages such as low cost, easy process and

can be deposited a large scale of thin films on different substrates at low deposition temperature including room temperature.

In recent work, ZnO thin film was deposited on glass substrate by using modified SILAR method. Two solutions bathes were used as an anionic bath and a cationic bath instead of using conventional SILAR. The nanorods-like ZnO thin film by using modified SILAR method was successfully prepared. The prepared film was annealed and then characterized by using X- ray diffraction (XRD), FESEM, EDS, UV-VIS spectroscopy, Raman and FTIR spectroscopy. The synthesized film was used as NO_2 gas sensing material and showed enhancing in the response as well as response/ recovery time as it is compared to that of recent literature survey.

Materials and methods

To synthesize the ZnO thin film by using modified SILAR method [17], Zinc acetate dehydrate $(Zn(CH_3CO_2)_2 \cdot 2H_2O)$ was used as precursors i.e. 0.1 M of zinc acetate was dissolved in 100 mL of distilled water. Next an equivalent of distilled water in another beaker was adjusted its pH up to 11.5 by adding ammonia solution. The stirrer of acetate solution was for 45 min at room temperature. After that the acetate solution and water heated up to 60 °C. The glass substrate was washed with a hot chromic acid then washed with detergent mixed with tap water then rinsed with acetone. Finally, it was washed with distilled water and dried at room temperature. The substrate was immersed in precursor solution then in distilled water at 60 °C for 30 s for each solution i.e. 1 cycle equals 1 min and the immersed cycles were continue 70 cycles. The prepared film was annealed for 2 h at 200 °C by using muffle furnace. After cooling it at the room temperature, the prepared film was taken to further characterizations.

Gas-sensing test

The gas sensing performance of ZnO film was studied by measuring the change in the resistance of the film with respect to the different NO_2 gas concentrations at 200 °C operating temperature by using a home built static gas sensing system. The system contains a sealed stainless steel test chamber with a volume of 250 cm^3 with supply of gas inlet (to insert gas) and outlet (to remove gas), and a flat heating plate with a temperature controller. A Keithely 6514 electrometer with a computer-controlled data gathering system was linked to the film sensor's external connections. A silver paste for conducting was fixed on both ends of film 1×2 cm^2 area, the film mounted on 2 probe sample holder, which was inserted in stainless steel test chamber. The gas response of sensor was calculated by using the relation:

$$S = \frac{R_g}{R_a}$$

Where R_a and R_g are resistances of the sensor in air and gas testing respectively.

Results and discussion

Structural and surface morphological studies

The crystal structure of nanorods ZnO thin film is analyzed by XRD pattern as shown in **Figure 1**. The peaks indexed to the wurtzite crystal structure (JCPDS card No.36-1451), without any secondary phase. No another side peaks are found which shows that prepared sample purity. In the figure, 9 peaks are observed at 31.80, 34.48, 36.29, 47.61, 56.66, 62.96, 66.51, 68.04 and 69.14 corresponding (100), (002), (101), (102), (110), (103), (200), (112), (201) diffraction planes respectively, with a lattice constant of a = 3.247 A° and c = 5.198 A°. The high intensity of peaks indicated high crystallinity. The average crystalline size can be calculated by using Deby-Scherrer equation.

$$D = \frac{K\lambda}{\beta \cos \theta_B}$$

Where D is crystalline size, K is the Scherrer constant, λ is the incident wavelength of X- ray (1.5406 A°), β is the full width at half maximum intensity, and θ_B is the diffraction angle. The calculated of average crystalline size is 17.24 nm.
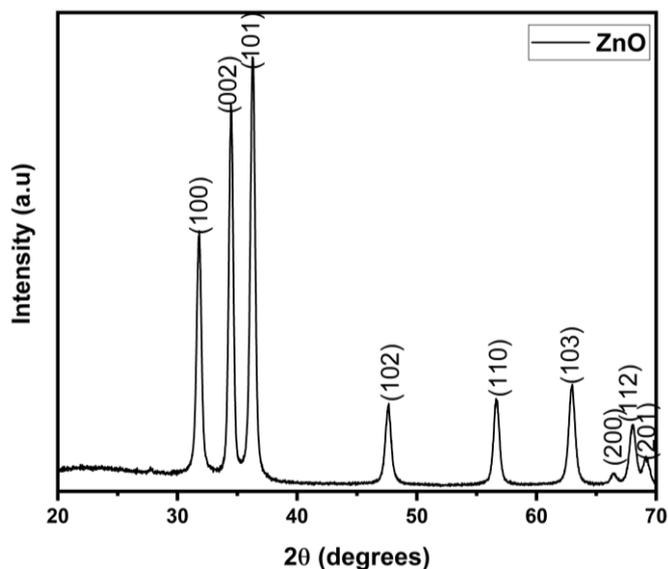
Figure 1 XRD patterns of ZnO thin film.

Figures **2(a)** and **2(b)** show FESEM morphology of ZnO thin film at different resolution. In the FESEM photograph, it is clear that the surface morphology of the sample is nanorods-like structure. The average length of nanorods is 2.6 μm. This nanorods structure plays an important role in gas sensor performance. The 1-dimensional structure only allows for 1 electron transit channel, which provides a free path for electron transport since the longer nanorods have a larger surface area. Thus, the sensitivity of nanorods is higher.

The chemical compositional of the prepared sample was analyzed by using EDS spectroscopy. **Figure 3** the EDS spectra illustrates the elements which is expected to form the sample such as Zn and O are observed.
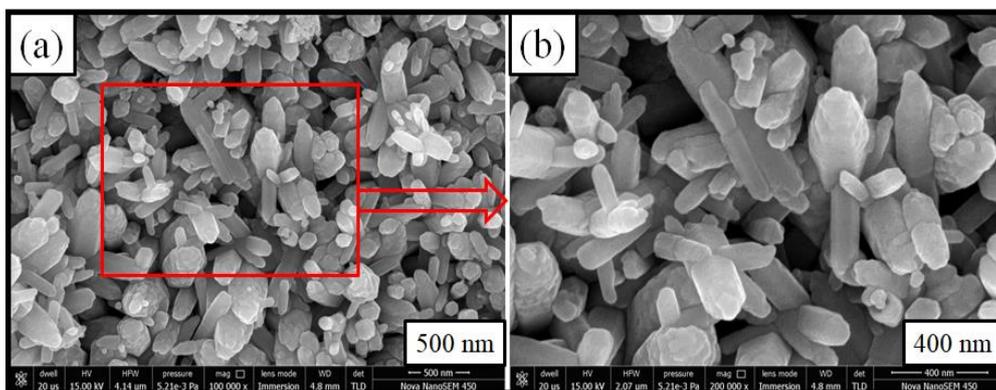

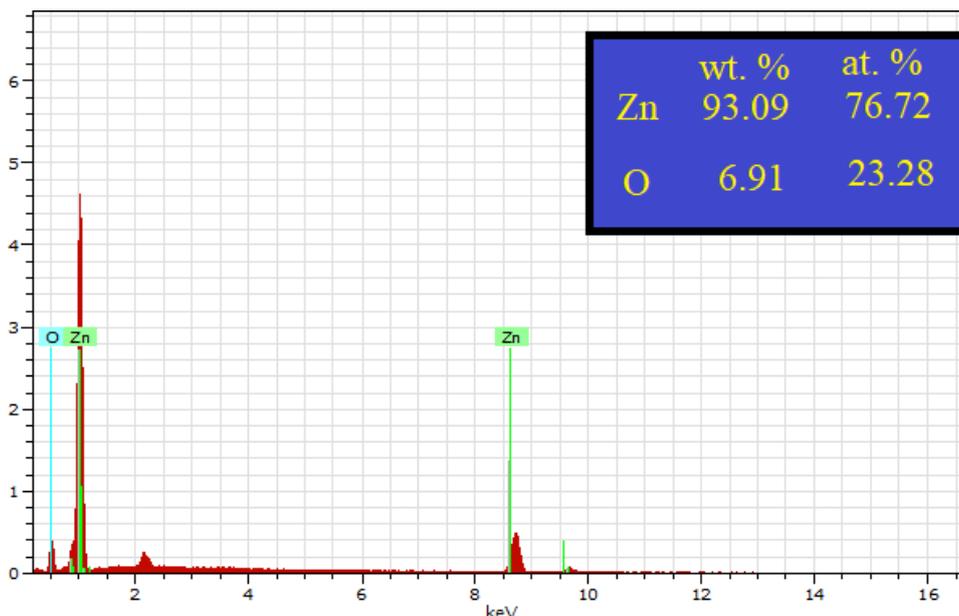**Figure 2** FESEM micrograph of ZnO thin film (a) 500 nm (b) 400 nm.

Figure 3 EDS spectra of ZnO thin film.

Optical study

UV-VIS analysis

Figure 4 shows the UV- visible spectra in the range (300 - 900 nm) of ZnO nanorods- like thin film, it is clear from the figure that the absorption band at 366 nm. The energy band gap of sample can be calculated from the relation:

$$\alpha h\nu = A\left(h\nu - E_g\right)^n$$

Where α is absorption coefficient, A is constant, n = ½ for allowed direct band gap and 2 for indirect band gap, $h\nu$ is the photon energy and E_g is optical energy band gap. The energy band gap (E_g) can be estimated from the Tauc plot as illustrated in inset figure in **Figure 4** by plotting $(\alpha h\nu)^2$ against $h\nu$ and the intercept the straight-line part with $h\nu$ axis, which found to be 3.17 eV.
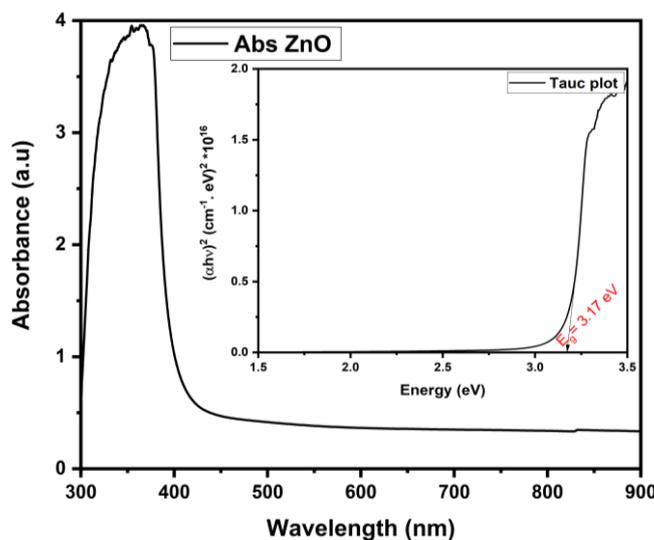

Figure 4 UV-VIS spectra of ZnO thin.

Raman analysis

The Raman spectra in the range of 200 - 800 cm^{-1} is illustrated in **Figure 5**. It can be seen from **Figure 5** the peak located at 436.9 cm^{-1} is attributed to E_2 (high) mode, which is the Raman active mode of wurtzite hexagonal ZnO structure [18-20]. The peaks observed at 332 and 581.7 cm^{-1} are due to E_{2H} - E_{2L}, and $E_{1(LO)}$ modes, respectively. The observed of $E_{1(LO)}$ at 581.7 cm^{-1} is attributed to oxygen vacancies [19,21]. The peak appearance at 407 cm^{-1} is assigned to $E_{1(TO)}$ mode [22]. The peak observed at 481 cm^{-1} may be attributed to surface phonon mode [20,23]. The peaks located at 276 and 648 cm^{-1} may be due to the silent $B_{1(LOW)}$ modes ($B_{1(L)}$ and TA + $B_{1(H)}$) [24].
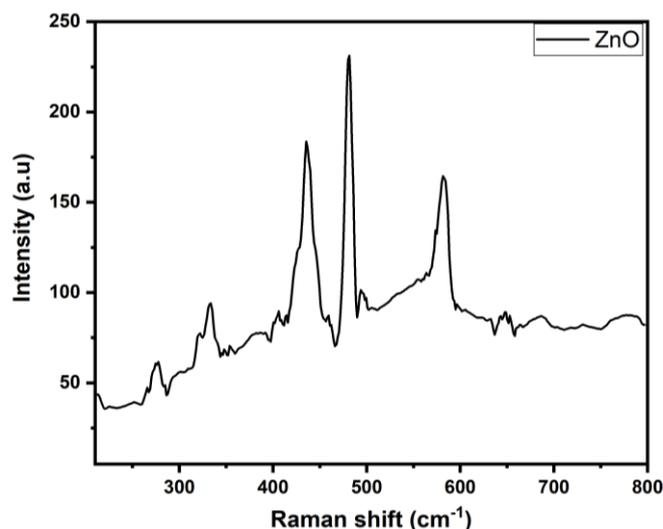

Figure 5 Raman spectra of ZnO thin film.

FT-IR analysis

Figure 6 shows the FTIR spectra of nanorods-like ZnO thin film measured in the range 4,000 - 650 cm^{-1}. The peaks observed around 3,700, 1,786 and 1,174 cm^{-1} are attributed to O─H stretching vibration mode due to adsorbed water on ZnO surface [25,26]. The peak at 2,973 cm^{-1} is C─H stretching vibration band [27]. The peak located at 2352 cm^{-1} is due to CO_2 coming from atmosphere [28,29]. The peaks at 1,323 and 1,479 cm^{-1} are assigned to C═O bending vibration and stretching vibration, respectively [27,29]. Finally, the peaks noticed in the range 1,000 - 650 cm^{-1} are attributed to the Zn─O stretching vibrations [26,30].
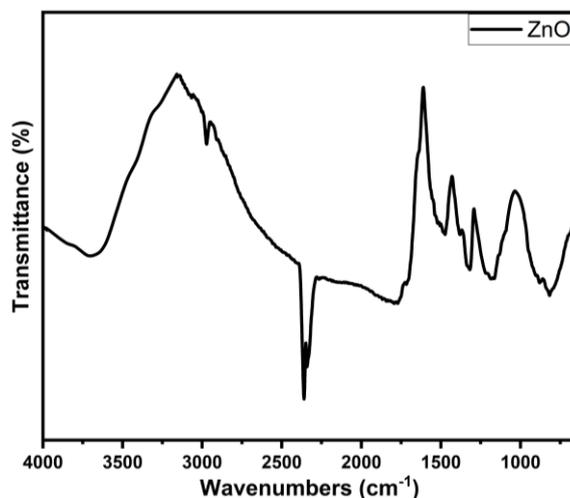

Figure 6 FT-IR spectra of ZnO thin film.

Gas sensing analysis

It is known that the chemiresistive metal oxide gas sensor works on the basis of the change in the electrical resistance of its surface during the process of adsorption and desorption of gas molecules. The gas sensing measurement of nanorods-like ZnO thin film was carried out by using home-built static gas sensing system.

Sensitivity

The sensitivity of ZnO film towards NO_2 gas was calculated by using the relation $S = R_g /R_a$, where R_g and R_a are the resistance of ZnO thin film with and without NO_2 gas exposed, respectively. **Figure 7** shows the resistance (kΩ) with time (s) of nanorods-like ZnO thin film at operating temperature (200 °C) for different NO_2 gas concentrations (10, 20, 40, 60 and 80 ppm). It is clear from the **Figure 7** that the resistance of ZnO thin film increased after exposed to NO_2 gas, this can be understood as a result of interaction of oxidizing gas (NO_2) with n-type ZnO thin film surface which leads to increase the height of depletion layer as well as increasing in resistance [31]. Furthermore, the increasing of thin film resistance and response ZnO thin film with increasing NO_2 concentrations were noticed, which can be attributed to the increasing in concentration that leads to increase interactivity of surface area with gas molecules [32]. **Figure 8** shows the responses of thin film towards different NO_2 concentrations at operating temperature 200 °C. The highest response at 200 °C can be understood as a result to enhancing the chemisorbed amount of NO_2 and increase of the surface reaction to overcome the activation energy barrier. It is clear from **Figure 8** that the nanorods-like ZnO thin film as sensing material showed a good response to low NO_2 gas concentration (10 ppm), which is around 1.37. It is noticed that the response increased with increase in the NO_2 gas concentrations. The obtained responses towards NO_2 concentrations (10, 20, 40, 60 and 80 ppm), were 1.37, 1.56, 1.79, 1.81 and 2.16, respectively. The highest response was found around 2.16 at 80 ppm gas concentration.

Response and recovery time

Response and recovery time are important as sensing parameters. The response time can be defined as the interval time taken from the moment which gas exposure until the resistance of surface sensing material reached 90 % of its steady resistance, whereas the recovery time is defined as the interval time taken from the moment which gas removed and the resistance of surface sensing material attained 10 % of its steady resistance. **Table 1** shows the sensitivity, response/ recovery time and steady state resistance for nanorods-like ZnO thin film at 200 °C operating temperature for different NO_2 concentrations.

Table 1 sensitivity, response/ recovery time and steady state resistance of nanorods-like ZnO thin film at 200 °C for different NO_2 concentrations.

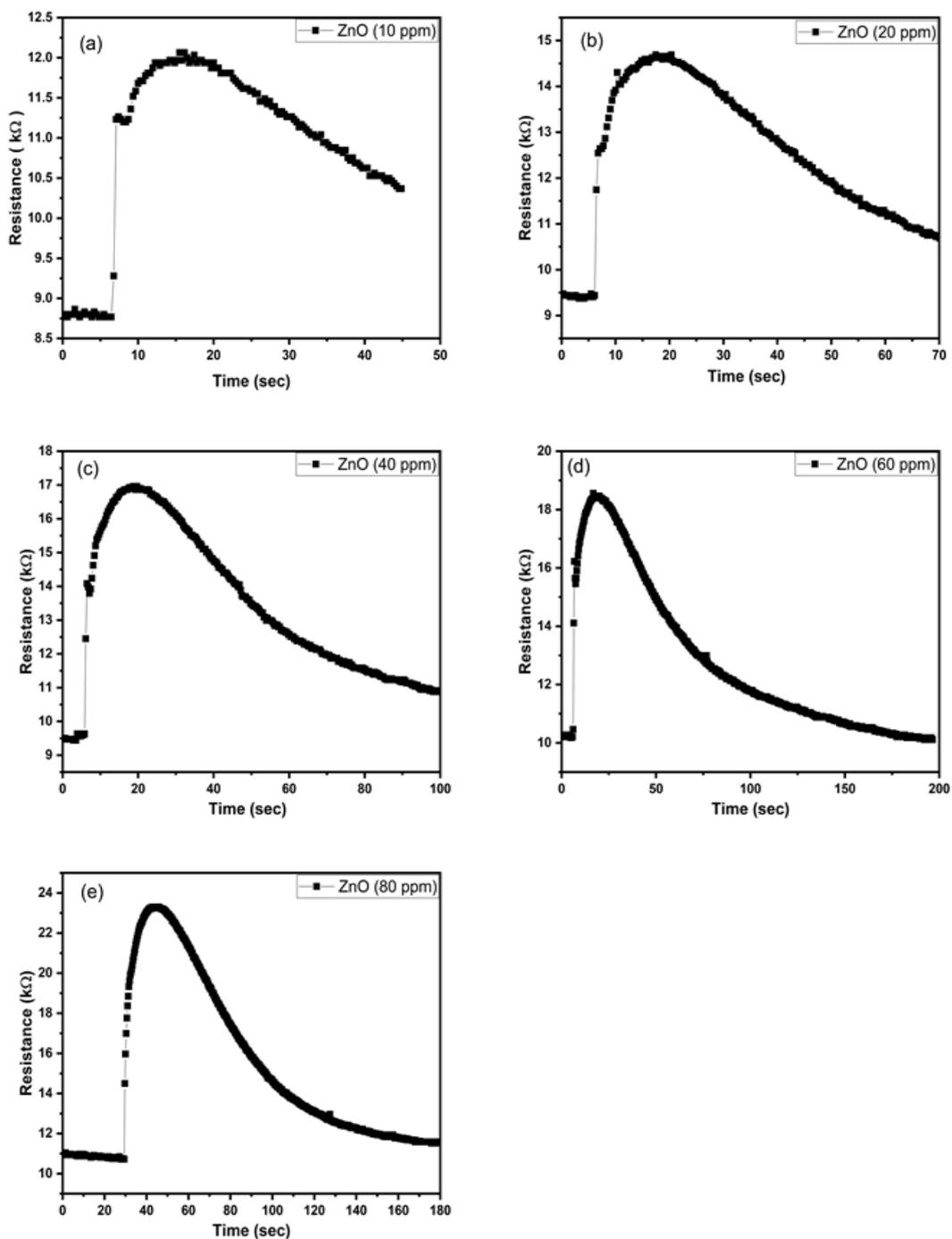| NO_2 concentration (ppm)	Gas response (R_g/R_a)	Response time (s)	Recovery time (s)	Steady state (kΩ)
20	1.56	2.36	48.74	14.58
40	1.79	2.93	72.8	16.997
60	1.81	2.79	75.35	18.55
80	2.16	4.46	74.15	23.43

Figure 7 Resistance vs time of ZnO nanorods-like at 200 °C, for: 10 ppm (a), 20 ppm (b), 40 ppm (c), 60 ppm (d), and 80 ppm (e).
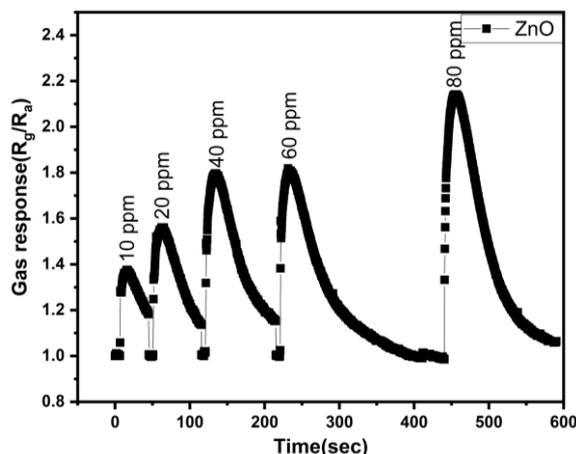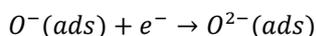
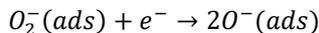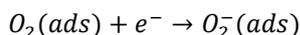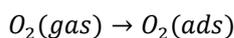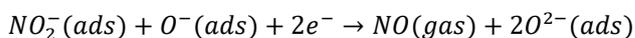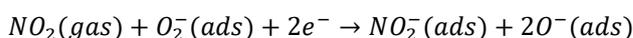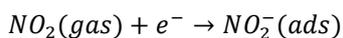**Figure 8** Response of ZnO nanorods-like towards different NO$_2$ gas concentrations.

Gas-sensing mechanism

The gas sensing mechanism of the zinc oxide-based sensor depends on the resistance change due to the phenomenon of chemical adsorption and adsorption of oxygen molecules in the surrounding air and the target gas on the sensor surface. At desired operating temperature, the formation of oxygen ions on the surface occurs due to the extraction of electrons from the conduction band of ZnO, which leads to an increase in the resistance of ZnO. The adsorbed oxygen according to the following reactions:

$$O_2(gas) \rightarrow O_2(ads)$$

$$O_2(ads) + e^- \rightarrow O_2^-(ads)$$

$$O_2^-(ads) + e^- \rightarrow 2O^-(ads)$$

$$O^-(ads) + e^- \rightarrow O^{2-}(ads)$$

It is known that zinc oxide is a semiconductor of n- type and NO$_2$ is oxidizing gas, so when NO$_2$ gas reacts with chemically adsorbed oxygen ions on the surface of ZnO, it works as acceptor and traps electrons from the ZnO surface, which lead to further increase of the resistance and barrier height [9,33] as flows reactions: [33]

$$NO_2(gas) + e^- \rightarrow NO_2^-(ads)$$

$$NO_2(gas) + O_2^-(ads) + 2e^- \rightarrow NO_2^-(ads) + 2O^-(ads)$$

$$NO_2^-(ads) + O^-(ads) + 2e^- \rightarrow NO(gas) + 2O^{2-}(ads)$$

Conclusions

In the present study, NO$_2$ gas sensing based on ZnO thin film deposited by modified SILAR method have been investigated. The XRD patterns showed that the obtained ZnO thin film exhibits hexagonal structure with a lattice constant of a = 3.247 A° and c = 5.198 A°. The average crystalline size calculated by using Deby-Scherrer equation was found to be 17.24 nm. The obtained morphological result by using FESEM reveals that this film contains nanorods-like morphology, which play a pivotal role in the gas adsorption desorption reaction, provides a higher surface-to-volume ratio and more surface area for sensing reaction, that leads to improvement in the gas sensing properties. UV-VIS result shows the absorption band at 366 nm and the energy bandgap was found 3.17 eV. Gas sensing study reveals that the prepared zinc oxide thin film respond to NO$_2$ (sensor response ~1.37 for 10 ppm NO$_2$ and the response increased with increase of NO$_2$ concentrations at optimum working temperature 200 °C), which are 1.56, 1.79, 1.81 and 2.16, when NO$_2$ concentrations 20, 40, 60, and 80 ppm, respectively. The increase of response by increasing NO$_2$ gas concentration is attributed to that the increasing in concentration that

leads to increase interactivity of surface area with gas molecules. Response/recovery time for 20, 40, 60 and 80 ppm are calculated to be 2.36/48.74 s, 2.93/72.8 s, 2.79/75.35 s and 4.46/74.15 s, respectively. The obtained results indicate that ZnO nanorods- like are promising materials to be used as an effective NO_2 gas sensor.

Acknowledgements

References

[1] VL Patil, SA Vanalakar, NL Tarwal, AP Patil, TD Dongale, JH Kim and PS Patil. Construction of Cu doped ZnO nanorods by chemical method for Low temperature detection of NO_2 gas. *Sens. Actuator A Phys*. 2019; **299**, 111611.

[2] DL Kamble, NS Harale, VL Patil, PS Patil and LD Kadam. Characterization and NO_2 gas sensing properties of spray pyrolyzed SnO_2 thin films. *J. Anal. Appl. Pyrolysis* 2017; **127**, 38-46.

[3] SA Vanalakar, VL Patil, NS Harale, SA Vhanalakar, MG Gang, JY Kim, PS Patil and JH Kim. Controlled growth of ZnO nanorod arrays via wet chemical route for NO_2 gas sensor applications. *Sens. Actuators B: Chem*. 2015; **221**, 1195-201.

[4] VL Patil, SA Vanalakar, SS Shendage, SP Patil, AS Kamble, N Tarwal, KK Sharma, JH Kim and PS Patil. Fabrication of nanogranular TiO2 thin films by SILAR technique. Application for NO_2 gas sensor. *Inorg. Nano-Met. Chem*. 2019; **49**, 191-7.

[5] VL Patil, SA Vanalakar, AS Kamble, SS Shendage, JH Kim and PS Patil. Farming of maize-like zinc oxide via a modified SILAR technique as a selective and sensitive nitrogen dioxide gas sensor. *RSC Adv*. 2016; **6**, 90916-22.

[6] RS Ganesh, VL Patil, E Durgadevi, M Navaneethan, S Ponnusamy, C Muthamizhchelvan, S Kawasaki, PS Patil and Y Hayakawa. Growth of Fe doped ZnO nanoellipsoids for selective NO_2 gas sensing application. *Chem. Phys. Lett*. 2019; **734**, 136725.

[7] M Kaur, M Shaheera, A Pathak, SC Gadkari and AK Debnath. Highly sensitive NO_2 sensor based on ZnO nanostructured thin film prepared by SILAR technique. *Sens. Actuators B: Chem*. 2021; **335**, 129678.

[8] H Wang, M Dai, Y Li, J Bai, Y Liu, Y Li, C Wang, F Liu and G Lu. The influence of different ZnO nanostructures on NO2 sensing performance. *Sens. Actuators B: Chem*. 2021; **329**, 129145.

[9] VS Bhati, M Hojamberdiev and M Kumar. Enhanced sensing performance of ZnO nanostructures-based gas sensors: A review. *Energy Rep*. 2020; **6**, 46-62.

[10] Q Qi, T Zhang, S Wang and X Zheng. Humidity sensing properties of KCl-doped ZnO nanofibers with super-rapid response and recovery. *Sens. Actuators B: Chem*. 2009; **137**, 649-55.

[11] R Kumar, O Al-Dossary, G Kumar and A Umar. Zinc oxide nanostructures for NO_2 gas–sensor applications: A review. *Nano-micro Lett*. 2015; **7**, 97-120.

[12] G Kaur, A Mitra and KL Yadav. Pulsed laser deposited Al-doped ZnO thin films for optical applications. *Prog. Nat. Sci. Mater. Int*. 2015; **25**, 12-21.

[13] A Goyal and S Kachhwaha. ZnO thin films preparation by spray pyrolysis and electrical characterization. *Mater. Lett*. 2012; **68**, 354-6.

[14] R Kara, L Mentar and A Azizi. Synthesis and characterization of Mg-doped ZnO thin-films electrochemically grown on FTO substrates for optoelectronic applications. *RSC Adv*. 2020; **10** 40467-79.

[15] PFH Inbaraj and JJ Prince. Optical and structural properties of Mg doped ZnO thin films by chemical bath deposition method. *J. Mater. Sci. Mater. Electron*. 2018; **29**, 935-43.

[16] KR Devi, G Selvan, M Karunakaran, K Kasirajan, LB Chandrasekar, M Shkir and S AlFaify. SILAR-coated Mg-doped ZnO thin films for ammonia vapor sensing applications. *J. Mater. Sci. Mater. Electron*. 2020; **31**, 10186-95.

[17] H Güney and D İskenderoğlu. Synthesis of MgO thin films grown by SILAR technique. *Ceram. Int*. 2018; **44**, 7788-93.

[18] M Zhao, X Wang, L Ning, H He, J Jia, L Zhang and X Li. Synthesis and optical properties of Mg-doped ZnO nanofibers prepared by electrospinning. *J. Alloys Compd*. 2010; **507**, 97-100.

[19]   M Sypniewska, R Szczesny, P Popielarski, K Strzalkowski and B Derkowska-Zielinska. Structural, morphological and photoluminescent properties of annealed ZnO thin layers obtained by the rapid sol-gel spin-coating method. *Opto-electron. Rev*. 2020; **28**, 182-90.

[20]   T Torchynska, B El Filali, JA Jaramillo Gomez, G Polupan, JL Ramírez García and L Shcherbyna. Raman scattering, emission, and deep defect evolution in ZnO: In thin films. *J. Vac. Sci. Technol. A: Vac. Surf. Films*. 2020; **38**, 063409.

[21]   M Amin, NA Shah, AS Bhatti and MA Malik. Effects of Mg doping on optical and CO gas sensing properties of sensitive ZnO nanobelts. *Cryst. Eng. Comm*. 2014; **16**, 6080-8.

[22]   CL Du, ZB Gu, MH Lu, J Wang, ST Zhang, J Zhao, GX Cheng, H Heng and YF Chen. Raman spectroscopy of (Mn, Co)-codoped ZnO films. *J. Appl. Phys.* 2006; **99**, 123515.

[23]   H Zhou, L Chen, V Malik, C Knies, DM Hofmann, KP Bhatti, S Chaudhary, PJ Klar, W Heimbrodt and C Klingshirn. Raman studies of ZnO: Co thin films. *Phys. Status Solidi A* 2007; **204**, 112-17.

[24]   PS Venkatesh, V Ramakrishnan and K Jeganathan. Raman silent modes in vertically aligned undoped ZnO nanorods. *Physica B Condens. Matter*. 2016; **481**, 204-8.

[25]   S Bhatia, N Verma and RK Bedi. Ethanol gas sensor based upon ZnO nanoparticles prepared by different techniques. *Results Phys*. 2017; **7**, 801-6.

[26]   RA Zargar, S Chackrabarti, S Joseph, MS Khan, R Husain and AK Hafiz. Synthesis and characterization of screen printed ZnO films for solar cell applications. *Optik* 2015; **126**, 4171-4.

[27]   V Khorramshahi, J Karamdel and R Yousefi. Acetic acid sensing of Mg-doped ZnO thin films fabricated by the sol-gel method. *J. Mater. Sci. Mater. Electron*. 2018; **29**, 14679-88.

[28]   S Bai, T Guo, D Li, R Luo, A Chen and CC Liu. Intrinsic sensing properties of the flower-like ZnO nanostructures. *Sens. Actuators B: Chem*. 2013; **182**, 747-54.

[29]   S Dinesh and RK Duchaniya. ZnO-CdS powder nanocomposite: synthesis, structural and optical characterization. *J. Nano- Electron. Phys.* 2013; **5**, 03014-5.

[30]   M Arshad, MM Ansari, AS Ahmed, P Tripathi, SSZ Ashraf, AH Naqvi and A Azam. Band gap engineering and enhanced photoluminescence of Mg doped ZnO nanoparticles synthesized by wet chemical route. *J. Lumin.* 2015; **161**, 275-80.

[31]   VL Patil, SA Vanalakar, PS Patil and JH Kim. Fabrication of nanostructured ZnO thin films based NO_2 gas sensor via SILAR technique. *Sens. Actuators B: Chem*. 2017; **239**, 1185-93.

[32]   NB Patil, AR Nimbalkar and MG Patil. ZnO thin film prepared by a sol-gel spin coating technique for NO_2 detection. *Mater. Sci. Eng. B*. 2018; **227**, 53-60.

[33]   VS Kamble, YH Navale, VB Patil, NK Desai and ST Salunkhe. Enhanced NO_2 gas sensing performance of Ni doped ZnO nanostructures. *J. Mater. Sci. Mater. Electron*. 2021; **32**, 2219-33.